Optical and Photocatalytic Measurements of Co-TiO2 Nanoparticle Thin Films

Article *in* Plasmonics · January 2018

DOI: 10.1007/s11468-018-0693-7

3 authors, including:

Mai Khalaf
Sohag University
17 PUBLICATIONS **68** CITATIONS
SEE PROFILE

Hany M. Abd El-Lateef
Sohag University
72 PUBLICATIONS **502** CITATIONS
SEE PROFILE

Plasmonics
https://doi.org/10.1007/s11468-018-0693-7

Optical and Photocatalytic Measurements of Co-TiO_2 Nanoparticle Thin Films

Mai M. Khalaf[1,2] · Hany M. Abd El-Lateef[1,2] · H. M. Ali[3]

Received: 8 August 2017 / Accepted: 3 January 2018

Abstract
Co-TiO_2 nanoparticle thin films were synthesized by sol-gel method. The structural properties of the synthesized sample were studied using FTIR, XRD, and TEM. XRD confirmed the presence of double-phase anatase/rutile for the TiO_2 nanoparticles. Effect of annealing temperature and exposure to microwave energy on the optical properties were studied for transparent conductive oxide (TCO) application. The optical energy gap and refractive index were determined. It was found that microwave treatment is an effective method for reinforcing optical properties of films. The photocatalytic properties were studied by determining the absorbance of methylene blue (MB) using UV source as a function of illumination time.

Keywords Sol-gel method · Optical materials · Thin films · Nanostructures · Photocatalytic measurements

Introduction

Titanium dioxide (TiO_2) has remarkable optical and electronic properties as a transparent conductive oxide (TCO) due to its high transparency and wide band gap energy (3.2 eV) [1], and it is considered one of the most promising photo-catalysts for decomposing atmospheric pollution, self-cleaning surfaces, and self-sterilization and antibacterial owing to its UV absorbance, relatively high efficiency, nontoxicity, inexpensive and abundant material, highly oxidizing power, and long-term chemical stability [2, 3]. These interesting combinations of useful properties make it also a competitive candidate for numerous applications, such as water splitting [4], gas sensors [5], protective sunscreens [6], and solar cell [7]. Otherwise, the electronic and optical characteristics of TCO films are highly sensitive to processing indices, such as type of dopants, heat treatment, and other deposition conditions [8].

✉ Hany M. Abd El-Lateef
hmahmed@kfu.edu.sa; hany_shubra@yahoo.co.uk

[1] Department of Chemistry, College of Science, King Faisal University, Al Hufuf, Al Hassa 31982, Saudi Arabia

[2] Chemistry Department, Faculty of Science, Sohag University, Sohag 82524, Egypt

[3] Physics Department, Faculty of Science, Sohag University, Sohag 82524, Egypt

Despite TiO_2 is widely used as a photocatalyst, there are still many efforts being made to improve its photocatalytic activity [2, 9]. Since TiO_2 is characterized by large optical energy gap, it needs higher energy for activation process, which can be achieved by ultraviolet illumination. The photocatalytic activity depends on the nature and extent of defects in the crystal [10], which may be achieved by doping techniques using either metallic dopants like Ag, Cu, Zn, and Co [11–13] or non-metallic dopants like nitrogen [14]. Doping lessens TiO_2 band gap which reduces the recombination rate of photogenerated electron–hole pairs [15]. Improvement of photocatalytic activity can be achieved under different conditions of preparation and irradiation and affected greatly by several parameters, including phase structure and crystalline size [16].

TiO_2 exists in three crystalline polymorphs: rutile (which crystallizes in the tetragonal form, the band gap is about 3 eV), anatase (crystallizes in the tetragonal, the band gap is about 3.2 eV), and brookite (crystallizes in the orthorhombic system, the band gap is about 3 eV) [17–19]. The anatase TiO_2 is preferable if used as photocatalytic cell and also suitable for use as gas sensors, solar cells, and multilayer optical coatings due to its high refractive index [20]. Rutile is the most thermodynamically stable and the densest; subsequently, it is an especially desirable oxide phase for optical functional implementations [21].

In this work, cobalt-doped titanium dioxide thin films were prepared by sol-gel procedure. Effect of annealing temperature and exposure to microwave energy were studied for

Published online: 13 January 2018

optical and solar cell applications. To the extent of our knowledge, there are no studies about the effect of microwave energy on the optical features of thin films. On other side, the photocatalytic properties were studied by determining the absorbance of methylene blue (MB) using UV source as a function of illumination time.

Experimental Section

Sol-Gel Preparation

The preparation of Co-TiO_2 nanoparticles by sol–gel method has been carried out in several steps presented in Fig. 1 as follows; a 67.5 ml of isopropanol (iPr-OH) (99%, Aldrich), was mixed with deionized water and allowed to stir for 20 min. Then, 7.4 ml of titanium isopropoxide (TTIP) as a Ti precursor (97%, Aldrich) was added by pipette to the beaker containing iPr-OH. The mixture was continually stirred using a magnetic stirrer after mixing and for a further 5 min after addition of the precursor. The pH of the solution was adjusted to 2 with HNO_3 (0.5 N). Cobalt nitrate as cobalt source was mixed together with titania sol followed by addition of 2 ml of acetyl acetone as capping agent under vigorous stirring for 2 h. The prepared cobalt-titanium hydroxide was aged overnight, dried for several hours at 100 °C, and annealed at various temperatures (200 ± 1300 ± 1400 ± 1 and 500 ± 1 °C) for 60 min.

Thin Film Preparation

Microscopic glass substrates were cleaned ultrasonically through Branson 1210 ultrasonic cleaner using both distilled water and acetone. The glass substrates were heated by hot plate at 100 °C for 5 min before deposition. The prepared Co-TiO_2 thin films were synthesized by dipping them in the solution for fixed intervals of dipping time. Then, films were dried at 60 °C in a muffled furnace for approximately 30 min.

Powder Characterization

Structural analysis of the prepared Co-TiO_2 powder was performed using an X-ray diffractometer (Phillips PW-1710) Cu-kα radiation (λ = 1.54056 Å) by changing the diffraction angle 2 from 4 to 80° by step width of 0.06. The FTIR spectra were measured for dried powder at different temperatures (200, 300, 400 and 500 °C) using FTIR spectrometer (BRUKER) in the domain 400–4000 cm^{-1}. Surface morphology of the films was analyzed by transmission electron microscopy (TEM) (model Jeol TEM-1230) at 100,000 magnifications and an acceleration voltage of 120 kV.

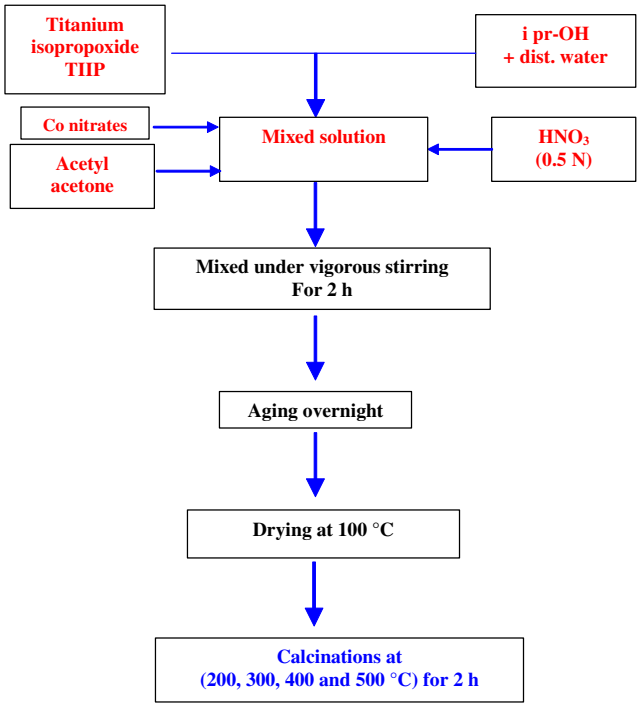

Fig. 1 Schematic process for preparation of Co-TiO_2

Optical Measurements

A Jasco V-570 UV–visible–NIR double beam spectrophotometer was utilized to record the reflection spectra and transmission over the wavelength range 200–2500 nm at normal incidence with a scan speed of 1000 nm min^{-1}. A further attachment model ISN-470 is provided for measuring the reflectivity of the films.

Film Annealing and Microwave Exposure

The prepared films were annealed at 100, 200, 300, 400, and 500 °C for 30 min in a fully controlled furnace. Another group of the prepared films was treated in microwave oven model No. MS-424EZ/01, with RF output microwave power of 900 W for t_M = 3, 6, 9, 12, and 15 min.

Photo-Catalytic Activity

The photo-catalytic properties of the prepared Co-TiO_2 film have been tested at room temperature by measuring the methylene blue (MB) decomposition ($C_{16}H_{18}ClN_3S \cdot xH_2O$). The film has been dipped into an aqueous solution of MB with a concentration of 1.0 mmol l^{-1} for 60 min then dried in air for 60 min in a dark venue. The film was illuminated by UV source (model Camag) for different times of t_{UV} = 5, 10, 15, 30, 60, and 90 min.

Result and Discussion

Figure 2 shows XRD patterns of Co-TiO_2 powders calcinated at 200, 300, and 500 °C. It is evident that the samples calcined at temperatures of 200 and 300 °C have amorphous structure. The amorphous nature of the samples can be attributed to large number of defect sites [22]. The sample calcined at 500 °C exhibits crystalline nature, and the obtained diffraction patterns were compared with database standards (JCPDS data card No. 46–1238). The prominent diffraction peaks (101), (103), (004), (200), (211), (204), (116), and (215) were at 25.27, 36.93, 37.89, 48.1, 54.58, 62.72, 68.9, and 75.09°, respectively, indicating the formation of anatase TiO_2 comparing with Card No. 35-0793 for Anatase TiO_2. Other diffraction peaks indicate the formation of TiO_2 in rutile structure (card No. 21-1276). The presence of anatase and rutile phase TiO_2 nanostructure is an interesting behavior due to the alteration in the crystal structure of the same material, which permits the electron transfer excited by ultraviolet light from anatase to rutile TiO_2 [23]. As the annealing temperature was increased to 500 °C, the peaks became more prominent, and this reveals that thermal treatment of the samples at higher temperature facilitates the development of rutile TiO_2 crystals.

The crystallite size (D) of Co-TiO_2 was calculated from the XRD spectra using Scherrer's equation [24],

$$D = \frac{0.9\lambda}{B\ \cos\ \theta_B} \quad (1)$$

where $\lambda = 1.54056$ Å and is the measured full width at half maximum (FWHM) at an angle of 2 in radian. Values of FWHM and the crystallite size are illustrated in Table 1. The average value of calculated crystallite size is in the range of 26.1 nm.

Figure 3 presents the FTIR spectra measured from 400 to 4000 cm^{-1} for Co-TiO_2 powders, calcined at different temperatures of 100, 200, 300, and 500 °C. A broad band at 2500–3600 cm^{-1} due to free H_2O molecules can be noticed [25, 26]. Observed bands were indicated around 3430 cm^{-1}, and those at 1530 cm^{-1} in the spectra are due to stretching and bending vibration of the hydrogen bonded -OH group of the adsorbed water molecules.

After calcinations, the intensity of these bands is decreased gradually and disappeared at 500 °C, indicating the removal of a large portion of the adsorbed water. Accordingly, the broad shoulders which extend from 900 to 400 cm^{-1} detect the existence of Ti-O-Ti vibrations. In samples at lower annealing temperatures, the shoulders are broader because of the presence of metal hydroxide Ti-OH [27]. The higher annealing temperatures lead to losing of water of hydroxyl surface groups to form metal–oxygen–metal links [28]. There is no peak at 2900 cm^{-1} for Co-TiO_2 calcined at 500 °C corresponding to -CH_3 and -CH_2 organic groups as a result of using isopropanol and acetyl acetone, which means all organic compounds are removed from the samples after calcinations.

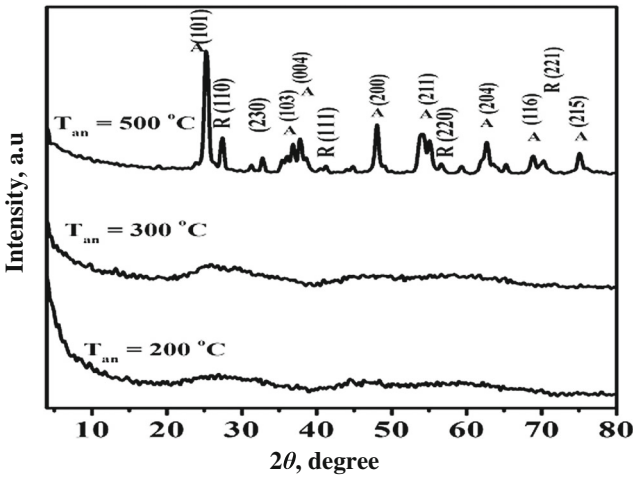

Fig. 2 The X-ray diffraction (XRD) patterns of Co-TiO_2 powders calcined at 200, 300, and 500 °C

Figure 4 shows TEM microphotographs obtained from Co-TiO_2 annealed at 500 °C. It could be found that a large number of crystalline grains appear in a structured matrix exhibited as spherical aggregates and the grains have a diameter in the range of 18–32 nm. As estimated from the TEM images, the crystalline grains are compatible with that obtained from XRD results which found to be in the range of 21–32 nm as indexed in Table 1.

The transmittance (T%) and reflection (R%) spectra of as deposited Co-TiO_2 and annealed films at different temperatures of T_{an} = 100, 200, 300, 400, and 500 °C for 30 min in the wavelength range from 200 to 2500 nm are presented in Fig. 5a,b. It is evident that the T% increased gradually as increment of the annealing temperature. The value of T% ~ 88% in the visible and near infrared regions of the spectrum was obtained for film annealed at 500 °C. The increase in transmittance can be attributed to the decrease of the number of water molecules and undesirable light impurity atoms in the sample. No considerable change in reflection was observed,

Table 1 The calculated FWHM and crystallite size D (nm) from the XRD patterns of Co-TiO_2 powder calcined at 500 °C

Peak		FWHM (n)	Crystallite size D (nm)
(101)	A-TiO_2	0.67	21.2
(110)	R-TiO_2	0.57	25.0
(230)	TiO_2	0.51	28.3
(103)	A-TiO_2	0.45	32.5
(004)	A-TiO_2	0.51	28.8
(200)	A-TiO_2	0.62	24.5
(204)	A-TiO_2	0.69	23.5

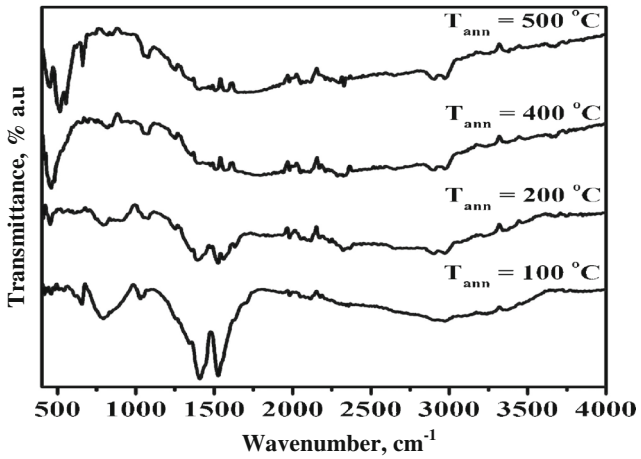

Fig. 3 The FTIR spectra of Co-TiO_2 powders calcined at different temperatures

indicating that the decrease in absorption is responsible for increasing the film transparency.

Another trial to improve the optical features of the prepared samples was performed by exposing the film to microwaves for different times $t_M = 3$, 6, 9, 12, and 15 min. A microwave oven with RF output power 900 W was used. The transmittance and reflectance spectra of Co-TiO_2 exposed to microwaves for different times are shown in Fig. 6a,b. The transmittance increased with an increase in time of exposure at the same time decreasing the reflectivity. The transmittance values were in the range of 81.0% and 84.0% in the visible and NIR regions for film exposed to microwaves for 15 min. No significant increase was found in transparency above 12 min.

The transmittance values obtained by exposing the Co-TiO_2 film to microwave power for 15 min are near than those obtained by annealing temperature at 400 °C for 30 min, confirming treatment by microwaves saves power and time.

The optical energy gap of Co-TiO_2 was determined using Tauc's equation by extrapolating the linear portion of the plots

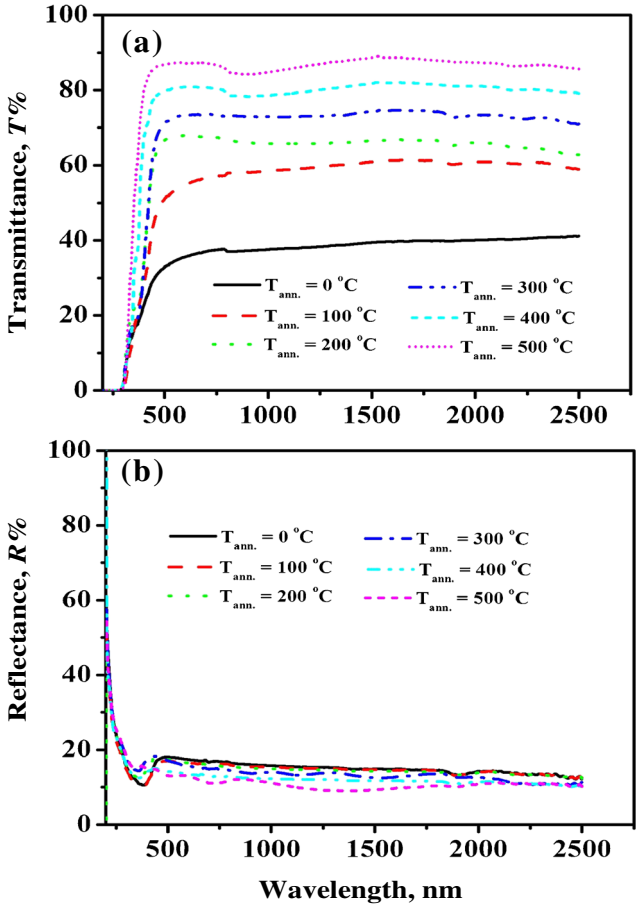

Fig. 5 The transmittance (**a**) and reflection (**b**) spectra of as-deposited Co-TiO_2 and annealed films at different temperatures for 30 min

of $(h)^2$ vs. h at $(h)^2 = 0$ [29]. The corresponding optical energy gap of as-deposited and annealed Co-TiO_2 is presented in Fig. 7a, whereas the optical energy gap of Co-TiO_2 exposed to microwave power for different times is shown in Fig. 7b. The figure shows that the as-deposited film has the lowest optical energy gap at ~2.93 eV, confirming that doping by

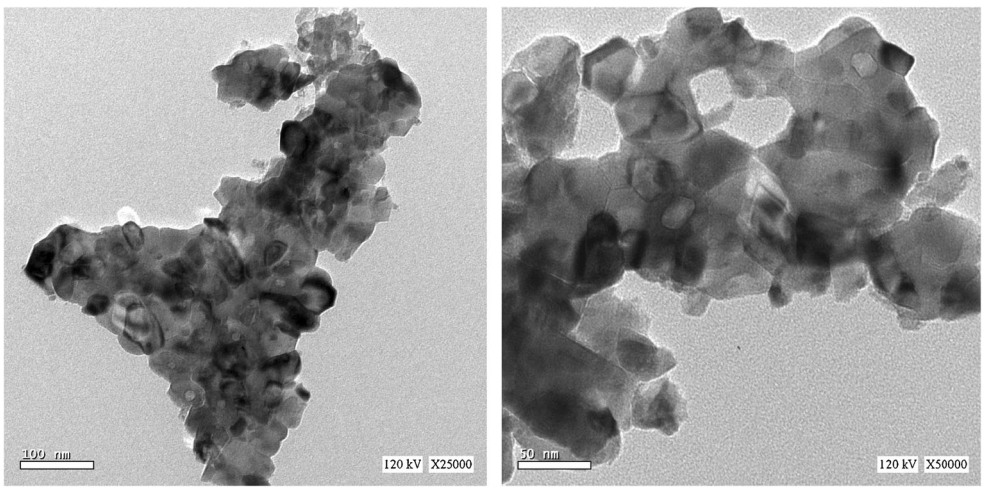

Fig. 4 TEM micrographs of powdered Co-TiO_2 annealed at 500 °C at magnifications 25,000× and 50,000×

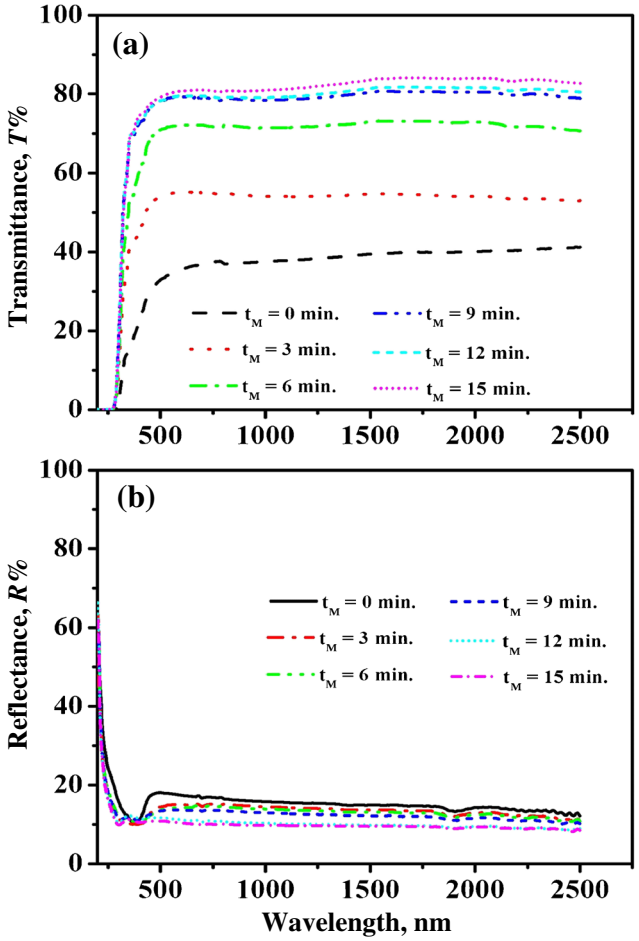

Fig. 6 Transmittance (**a**) and reflectance (**b**) spectra of Co-TiO_2 film exposed to microwave power for different times

Co lessens the band gap of TiO_2. It is also observed that the optical gap energy increment increases with either the time of exposure to microwave power or the temperature of annealing. The maximum values of optical energy gap obtained are 3.2 and 3.37 eV for film annealed at 500 °C and film exposed to microwave for 15 min, respectively. The increase of optical energy gap may be due to the decrease in density of localized states. The impurities are gradually decreased either by annealing temperature or by exposing the film to microwave power.

The refractive index of a material is the key factor for device design [30]. The refractive index in visible region of Co-TiO_2 films annealed at different temperatures and exposed to microwave power for different times is presented in Fig. 8a,b. The figure shows that the refractive index decreases with increase of temperature of annealing or time of exposure to microwave power. The average value of as-deposited Co-TiO_2 thin film is about 2.41 that decreases to 2.07 for film annealed at 500 °C and about 1.94 for film exposed to microwave power for 15 min.

The obtained data of average refractive index were listed in Table 2. The data are in good agreement with those obtained by Assim [31] for $TiO_{1.7}$ deposited by electron beam gun. The same trend was obtained by Xue et al. [32] for ZnO films. It was discussed that the decrease in refractive index with an increase in the annealing temperature is due to the decrease of optical absorption. The small value of refractive index can be attributed to the improvement of transparency of the films [33].

Figure 9a,b presents the variation of absorption spectra and MB degradation of as deposited Co-TiO_2 thin film after dipping in MB as a function of wavelength before and after illumination by UV source. It can be observed that the absorption decreases as illumination time increases from 5 to 90 min. The dye degradation percentage of 60 was obtained after 90 min from the initial 1 mmol/L dye concentration used under UV spectrum for photocatalytic activity. This can be interpreted as the amount of dye uptake increases with the increase of illumination time. It can be observed that Co-TiO_2 is of higher reactivity for the photocatalytic degradation of MB. The higher reactivity appears to be mainly linked to the presence of anatase phase of the sample. This higher photocatalytic performance

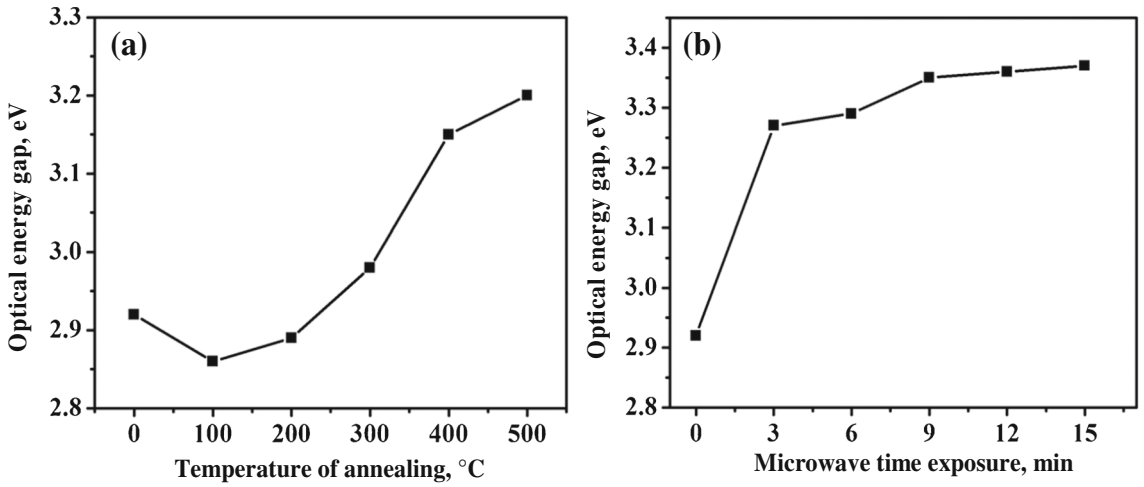

Fig. 7 Optical energy gap of Co-TiO_2 films (**a**) annealed at different temperatures and (**b**) exposed to microwave power for different times

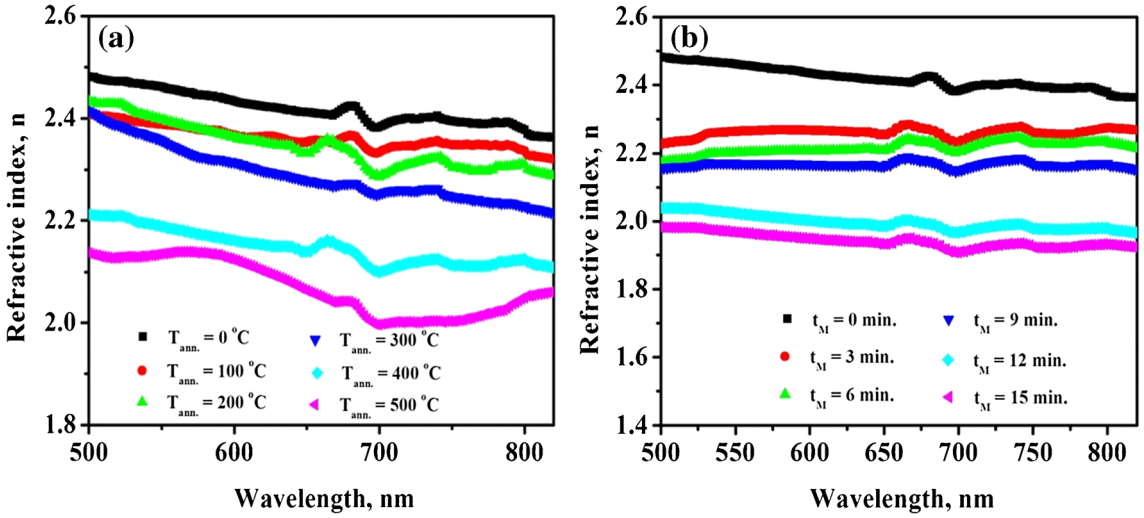

Fig. 8 Wavelength dependence of refractive index of Co-TiO_2 films (**a**) annealed at different temperatures and (**b**) exposed to microwave power for different times

under UV irradiation is in good agreement with the optical data, which has the lowest optical energy gap at ~2.93 eV giving rise to reduce the band gap of TiO_2. Therefore, the presence of Co as dopant improves the photochemical properties of the sample by reducing the recombination of photogenerated electrons and holes is questionable [34, 35].

Conclusions

Co-TiO_2 thin films were prepared by sol-gel method. The structural properties of the prepared sample were studied using FTIR, XRD, and TEM. The XRD confirmed the presence of double-phase anatase/rutile for the TiO_2, and average value of calculated crystallite size is in the range of 26.1 nm. Effect of annealing temperature and exposure to microwave energy on the optical properties were studied for transparent conductive oxide (TCO) application.

Transmittance values of ~88% for annealed film at 500 °C and about 81% and 84% in the visible and near infrared regions, respectively, for exposed film to microwave power for 15 min were obtained. The obtained transmittance value at ~81% in the visible region obtained by exposing the Co-TiO_2 film to microwave power for 15 min was also obtained by annealing temperature at 400 °C for 30 min, confirming that treatment by microwaves is an effective method for enhancing the optical properties and saves power and time.

Table 2 The average values of refractive index in the visible region for Co-TiO_2 annealed at different temperatures and exposed to microwave power for different times

T_{ann} (°C)	n	t_M (min)	n
0	2.42	0	2.42
100	2.36	3	2.26
200	2.35	6	2.22
300	2.29	9	2.17
400	2.15	12	2.00
500	2.07	15	1.94

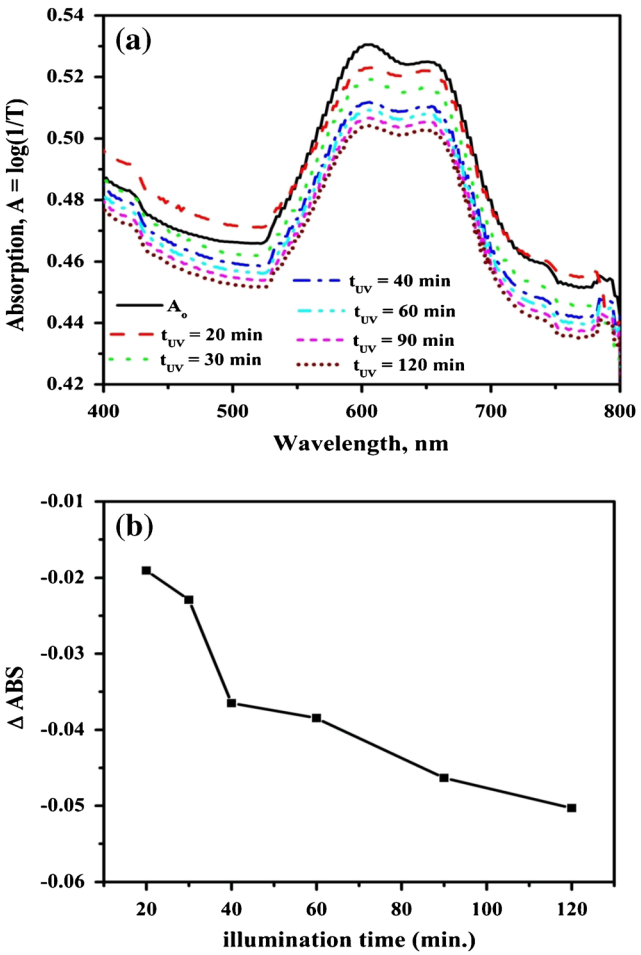

Fig. 9 MB absorption spectra of as-deposited Co-TiO_2 thin film (**a**) and the variation of the absorption degradation at 600 nm by MB as a function of illumination time (**b**)

The optical energy gap of Co-TiO_2 film was determined using Tauc's equation. It was found that the as-deposited film has the lowest energy gap at ~2.93 eV, confirming that doping by Co lessens the band gap of TiO_2. The maximum values of ~3.2 and 3.37 eV were obtained for film annealed at 500 °C and film exposed to microwave for 15 min, respectively.

The refractive index of annealed and exposed film to microwave was determined. It was found that the refractive index decreases as the temperature of annealing or time of exposure to microwave power increases. The as-deposited Co-TiO_2 has a photocatalytic activity for color-fading of MB. The dye degradation percentage of 60 was obtained after 90 min from the initial 1 mmol/l dye concentration used under UV spectrum for photocatalytic activity.

References

1. Ali HM, Abou-Mesalam MM, El-Shorbagy MM (2010) Structure and optical properties of chemically synthesized titanium oxide deposited by evaporation technique. J Phys Chem Solids 71(1): 51–55. https://doi.org/10.1016/j.jpcs.2009.10.008
2. Grabowska E, Zaleska A, Sobczak JW, Gazda M, Hupka J (2009) Boron-doped TiO_2: characteristics and photoactivity under visible light. Procedia Chem 1(2):1553–1559. https://doi.org/10.1016/j.proche.2009.11.003
3. Yonemochi S, Sugiyama A, Kawamura K, Nagoya T, Aogaki R (2004) Fabrication of TiO_2 composite materials for air purification by magnetic field effect and electrocodeposition. J Appl Electrochem 34(12):1279–1285. https://doi.org/10.1007/s10800-004-1762-5
4. Fujihara K, Ohno T, Matsumura M (1998) Splitting of water by electrochemical combination of twophotocatalytic reactions on TiO_2 particles. J Chem Soc 94:3705–3709. https://doi.org/10.1039/A806398B
5. Tian WC, Ho YH, Chen CH, Kuo CY (2013) Sensing performance of precisely ordered TiO_2 nanowire gas sensors fabricated by electron-beam lithography. Sensors 13(1):865–874. https://doi.org/10.3390/s130100865
6. Assim EM (2008) Optical constants of titanium monoxide TiO thin films. J Alloy Compd 465(1-2):1–7. https://doi.org/10.1016/j.jallcom.2007.10.059
7. Szpakolski K, Latham K, Rix C, Rani RA, Kourosh (2013) Silane: a new linker for chromophores in dyesensitised solar cells. Polyhedron 52:719–732. https://doi.org/10.1016/j.poly.2012.07.078
8. Ali HM, Mohamed HA, Mohamed SH (2005) Enhancement of the optical and electrical properties of ITO thin films deposited by electron beam evaporation technique. Eur Phys J Appl Phys 31(2):87–93. https://doi.org/10.1051/epjap:2005044
9. Ubonchonlakate K, Sikong L, Saito F (2012) Photocatalytic disinfection of P. aeruginosa bacterial Ag-doped TiO_2 film. Procedia Eng 32:656–662. https://doi.org/10.1016/j.proeng.2012.01.1323
10. Karunakaran C, Vinayagamoorthy P, Jayabharathi J (2013) Electrical, optical and photocatalytic properties of polyethylene glycol-assisted sol–gel synthesized Mn-doped TiO_2/ZnO core–shell nanoparticles. Superlattice Microst 64:569–580. https://doi.org/10.1016/j.spmi.2013.10.021
11. Kobwittaya K, Sirivithayapakorn S (2014) Photocatalytic reduction of nitrate over TiO_2 and Ag-modified TiO_2. J Saudi Chem Soc 18(4):291–298. https://doi.org/10.1016/j.jscs.2014.02.001
12. Munusamy S, Aparna RS, Prasad RG (2013) Photocatalytic effect of TiO_2 and the effect of dopants on degradation of brilliant green. Sustain Chem Process 1(1):4. https://doi.org/10.1186/2043-7129-1-4
13. Zuo Z, Huang W, Han P, Li Z (2009) Theoretical and experimental investigation of the influence of Co content on the titanium dioxide phase transition. Solid State Commun 149(47–48):2139–2142. https://doi.org/10.1016/j.ssc.2009.09.027
14. Cabrera RQ, Vazquez CS, Darr JA, Parkin IP (2014) Critical influence of surface nitrogen species on the activity of N-doped TiO_2 thin-films during photodegradation of stearic acid under UV light irradiation. Appl Catal B-Environ 160:582–588. https://doi.org/10.1016/j.apcatb.2014.06.010
15. Khairy M, Zakaria W (2014) Effect of metal-doping of TiO_2 nanoparticles on their photocatalytic activities toward removal of organic dyes. Egypt J Pet 23(4):419–426. https://doi.org/10.1016/j.ejpe.2014.09.010
16. Bouzaida I, Ferronato C, Chovelon JM, Rammah ME, Herrmann JM (2004) Heterogeneous photocatalytic degradation of the anthraquinonic dye, Acid Blue 25 (AB25): a kinetic approach. J Photochem Photobiol A Chem 168(1-2):23–30. https://doi.org/10.1016/j.jphotochem.2004.05.008
17. Asahi R, Taga Y, Mannstadt W, Freeman AJ (2000) Electronic and optical properties of anatase TiO_2. Phys Rev B Condens Matter 61: 7459–7465. https://doi.org/10.1103/PhysRevB.61.7459
18. Amtout A, Leonelli R (1995) Optical properties of rutile near its fundamental band gap. Phys Rev B Condens Matter 51:6842–6851. https://doi.org/10.1103/PhysRevB.51.6842
19. Koelsch M, Cassaignon S, Thanh Minh CT, Guillemoles J-F, Jolivet J-P (2004) Electrochemical comparative study of titania (anatase, brookite and rutile) nanoparticles synthesized in aqueous medium. Thin Solid Films 451:86–92. https://doi.org/10.1016/j.tsf.2003.11.150
20. Zribi M, Kanzari M, Rezig B (2008) Structural, morphological and optical properties of thermal annealed TiO thin films. Thin Solid Films 516(7):1476–1479. https://doi.org/10.1016/j.tsf.2007.07.195
21. Mohamed SH, Shaaban ER (2011) Microstructural, optical and photocatalytic properties of CdS doped TiO_2 thin films. Physica B 406(22):4327–4331. https://doi.org/10.1016/j.physb.2011.08.084
22. Balasubramanian A, Radahakrishnan M, Balasubramanian C (1982) Electrical properties of electron-beam-evaporated indium oxide thin films. Thin Solid Films 91(1):71–79. https://doi.org/10.1016/0040-6090(82)90125-0
23. Liu Z, Zhang X, Nishimoto S, Jin M, Tryk DA, Murakami T, Fujishima A (2007) Anatase TiO_2 nanoparticles on rutile TiO_2 nanorods: a heterogeneous nanostructure via layer-by-layer assembly. Langmuir 23(22):10916–10919. https://doi.org/10.1021/la7018023
24. Cullity BD (1979) Elements of X-ray diffraction, 2nd edn. Addison-Wesley, Reading, p 102
25. Nakamoto K (1978) Infrared and Raman spectra of inorganic and coordination compound. John Wiley and Sons, New York
26. Nyquist RN, Kagel RO (1997) Infrared and Raman spectra of inorganic compounds and organic salts. Academic Press, New York
27. Zou H, Lin YS (2004) Structural and surface chemical properties of sol–gel derived TiO_2–ZrO_2 oxides. Appl Catal A Gen 265(1):35–42. https://doi.org/10.1016/j.apcata.2004.01.015
28. Fu X, Clark LA, Yang Q, Anderson MA (1996) Enhanced photocatalytic performance of titania-based binary metal oxides: TiO_2/SiO_2 and TiO_2/ZrO_2. Environ Sci Technol 30(2):647–653. https://doi.org/10.1021/es950391v
29. Klug HP, Alexander LE (1970) X-ray diffraction procedures. Wiley, New York
30. Neumann H, Horig W, Reccius E, Sobotta H, Schumann B, Kuhn G (1979) Growth and optical properties of $CuGaTe_2$ thin films. Thin Solid Films 61(1):13–22. https://doi.org/10.1016/0040-6090(79)90494-2

31. Assim EM (2008) Optical constants of TiO1.7 thin films deposited by electron beam gun. J Alloy Compd 463(1-2):55–61. https://doi.org/10.1016/j.jallcom.2007.09.034
32. Xue SW, Zu XT, Zhou WL, Deng HX, Xiang X, Zhang L, Deng H (2008) Effects of post-thermal annealing on the optical constants of ZnO thin film. J Alloy Compd 448(1-2):21–26. https://doi.org/10.1016/j.jallcom.2006.10.076
33. Sun J, Gerberich WW, Francis LF (2007) Transparent, conductive polymer blend coatings from latex-based dispersions. Prog Org Coat 59(2):115–121. https://doi.org/10.1016/j.porgcoat.2007.01.019
34. Murakami SY, Kominami H, Kera Y, Ikeda S, Noguchi H, Uosaki K, Ohtani B (2007) Evaluation of electron-hole recombination properties of titanium (IV) oxide particles with high photocatalytic activity. Res Chem Intermed 33(3-5):285–296. https://doi.org/10.1163/156856707779238612
35. Ou C-C, Yang C-S, Lin S-H (2011) Selective photo-degradation of Rhodamine B over zirconia incorporated titania nanoparticles: a quantitative approach. Cat Sci Technol 1(2):295. https://doi.org/10.1039/c0cy00019a